compounds

MDPI

Article

Different Chain Length Tannic Acid Preparations as Coating Agents for Zein Nanoparticles

Sadeepa Y. Mallikarachchi, Nancy C. Rotich, Emma Gordon and Ann E. Hagerman *

Department of Chemistry & Biochemistry, Miami University, Oxford, OH 45056, USA; malliksy@miamioh.edu (S.Y.M.); chepchnr@miamioh.edu (N.C.R.); gordonea@miamioh.edu (E.G.)
* Correspondence: hagermae@miamioh.edu; Tel.: +1-513-529-2827

Abstract: Proteins that are amphiphilic and have low water solubility can self-assemble into nanoparticles useful in food science, pharmaceutical science, or biotechnology. However, protein nanoparticles exhibit drawbacks such as low stability unless the particles are coated. In the current study, tannic acid is the coating agent for nanoparticles synthesized from the protein zein. Tannic acid is a hydrolyzable tannin comprising a polyol esterified with galloyl residues. The nominal molecular formula of tannic acid ($C_{76}H_{52}O_{46}$) suggests the material is decagalloyl glucose, obscuring its complex composition as a mixture of galloyl esters of glucose. We prepared hollow zein nanoparticles and coated them with tannic acid preparations that had short or long galloyl ester chains. The % α-helix of zein in nanoparticles is lower than in native zein but there is no effect of coating the particles with tannic acid. Interactions between the tannic acid and the zein slightly perturb the IR spectrum of the protein but there is no effect of galloyl chain length. We confirmed that tannic acid-coated particles have a more negative zeta potential, suggesting greater stability compared to uncoated particles. Coating with longer chain length tannic acid reduces particle diameter and tends to decrease polydispersity but does not change particle digestibility. Coating with shorter galloyl chain length tannic acid tends not to change particle diameter, reduces polydispersity of the particles, and stabilizes particles to enzymatic digestion. Tannic acid is a naturally occurring tunable coating for nanoparticles that can be used to adjust properties such as particle size, polydispersity, and digestibility for specific purposes.

Keywords: tannin; polyphenol; protein precipitation; digestibility; pentagalloyl glucose; multivalent protein binding

Citation: Mallikarachchi, S.Y.; Rotich, N.C.; Gordon, E.; Hagerman, A.E. Different Chain Length Tannic Acid Preparations as Coating Agents for Zein Nanoparticles. *Compounds* **2024**, *4*, 401–414. https://doi.org/10.3390/compounds4020024

Academic Editors: Jorge F. B. Pereira and Cassamo U. Mussagy

Received: 11 March 2024
Revised: 21 May 2024
Accepted: 4 June 2024
Published: 13 June 2024

1. Introduction

Biodegradable nanoparticles may have diverse applications for drug delivery, food modifications, manufacturing, and biotechnology. For biological applications, nanoparticles are attractive due to their submicron sizes that lead to relatively higher intracellular uptake compared to microparticles [1]. Efficiency of cargo release is inversely proportional to particle size because release depends on surface area and proximity of the encapsulated material to the particle surface, so controlling particle size is important [2,3]. Compared to delivery systems such as emulsions, lipid nanoparticles, liposomes or microcapsules, biopolymer nanoparticles have favorable qualities including biocompatibility and biomimetic characteristics [4].

Proteins and polysaccharides are widely used to create biopolymer nanoparticles due to low toxicity, biodegradability, and availability as a commodity [5]. In particular, plant proteins are safe due to their minimal potential to provoke zoonotic disease transmission [6]. Zein, an alcohol-soluble protein (prolamin) is the major storage protein in maize endosperm cells [7]. This protein is amphiphilic because 50% of its amino acids are hydrophobic. Zein self-assembles into nanoparticles and can be developed as a delivery vehicle for hydrophobic molecules [8].

Both solid and hollow zein nanoparticles have been proposed for delivery applications. Although hollow particles have more potential to load cargo, they are more difficult to synthesize than solid particles [6]. Hollow nanoparticles are prepared by adding materials to create cavities in the particle either during or after particle synthesis. A novel method that uses sodium carbonate (Na_2CO_3) as a sacrificial template was developed by Xu and colleagues [6]. While zein dissolves in aqueous ethanol, sodium carbonate has limited solubility in organic-modified solutions. In 35% ethanol, carbonate forms particles that serve as templates for protein deposition. Water is added to dissolve the template and leave the protein nanoparticle suspended in basic solution. This "anti-solvent process" is a simple and effective method for producing zein nanoparticles (ZNP) [6].

To deliver their contents by oral administration, nanoparticles must be stable under gastrointestinal conditions comprising salts, extreme pH values and digestive enzymes. Protein nanoparticles may be more or less stable than the parent protein. For example, although zein has relatively low digestibility [9], unmodified ZNP aggregated and were hydrolyzed under gastrointestinal conditions [10]. Strategies such as surface coating or crosslinking with a polymer have demonstrated promising results including improved particle stability, delivery potential and rate of drug release [10,11]. Tannic acid (TA) is a biologically derived polymer that has been tested as a coating agent for protein nanoparticles [7].

Tannic acid, a commercially available hydrolyzable tannin, binds to and precipitates protein via hydrogen bonding, hydrophobic, and sometimes covalent interactions [12,13]. Tannic acid is often used as a stabilizing agent for protein-containing foods, beverages and pharmaceuticals [14–16]. It can also be used to fabricate hydrogels [17], thin films [18], and nanoparticles. Zein nanoparticles that are coated with TA are reported to be more resistant to digestion than uncoated ZNP [7]. Moreover, coating nanoparticles with TA has the potential to co-deliver health benefits associated with some polyphenols such as antibacterial, anticarcinogenic, antimutagenic, anti-allergic, anti-inflammatory or antihypertensive activity [19,20]. Despite these promising features of TA-coated protein nanoparticles, lack of understanding of how the galloyl chain length of TA preparations affects their function in nanoparticles is a research gap that limits our use of these systems.

Commercially available TA is not a pure compound. It is a mixture of galloyl esters of a core polyol, usually glucose, with different degrees and positions of esterification based on the botanical source and purification steps used by different suppliers (Figure 1) [21–23]. Preparations from some plant sources can contain rearrangement products such as castalagin/vescalagin. The nominal molecular weight and formula of TA that is provided by most suppliers ($C_{76}H_{52}O_{46}$, 1701 g/mol) is representative of the mixture but is not specific to a given preparation. Analysis with HPLC provides specific compositional information and reveals the heterogeneity of commercial supplies [21]. We hypothesize that the galloyl chain length of TA affects the properties of TA-coated ZNP, including their size, polydispersity index, zeta potential, morphology, and digestibility.

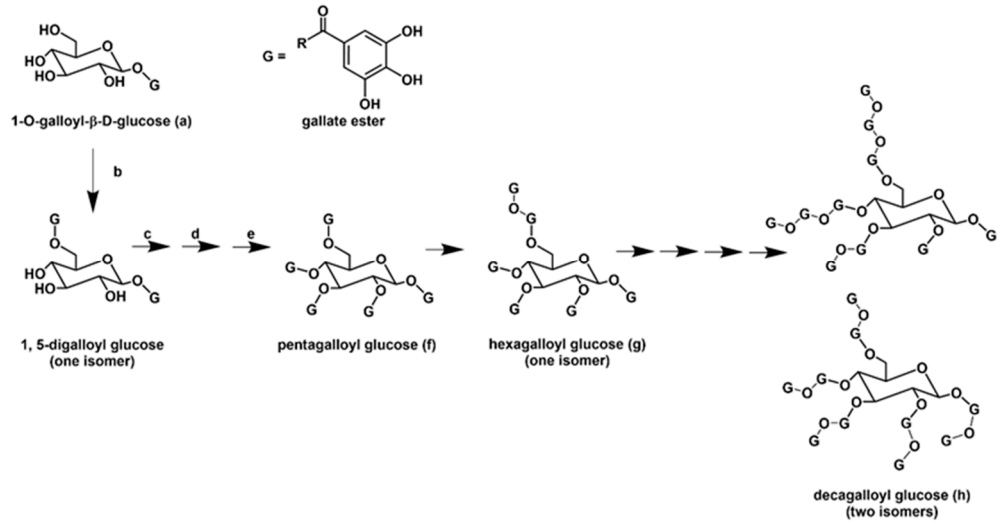

Figure 1. Biosynthetic basis for the variable galloyl chain length of commercial tannic acid preparations. In plants, 1-O-galloyl-β-D-glucose (monogalloyl glucose, glucogallin) (a) is esterified in a stepwise fashion (b–e) to produce a series of short chain-length galloyl esters [24]. The central metabolite pentagalloyl glucose (1,2,3,4,6-penta-O-galloyl-β-D-glucose) (f) is esterified at all five glucose OH groups, and subsequent steps add galloyl groups as depsides to generate medium chain-length (g) and long chain-length (h) galloyl esters. Positional isomers like those illustrated for decagalloyl glucose (h) add further structural diversity. Tannic acid is nominally comprised of decagalloyl glucose (h) ($C_{76}H_{52}O_{46}$) but HPLC analysis reveals that different commercial preparations are mixtures of many biosynthetic intermediates and isomers.

2. Materials and Methods

2.1. Materials

Zein was obtained from Sigma-Aldrich (St. Louis, MO, USA). Tannic acids were obtained from several suppliers: ACR was from Acros Organics (Geel, Belgium), MAL was from Mallinckrodt Chemicals (Paris, KY, USA), GFS was from GFS Chemicals (Powell, OH, USA), and FIS was from Fisher Scientific (Fairlawn, NJ, USA). Pentagalloyl glucose (PGG) was synthesized in our lab from TA and its purity and structure were confirmed by proton NMR and ESI-MS [25]. Chymotrypsin and bovine serum albumin (BSA) were from Sigma-Aldrich (St. Louis, MO, USA), and 4-(2-aminoethyl) benzenesulfonyl fluoride hydrochloride (AEBSF) protease inhibitor was from ThermoFisher (Waltham, MA, USA). Solutions were prepared with nanopure water or HPLC grade solvents. All other chemicals were reagent, HPLC, or electrophoresis grade.

2.2. Methods

2.2.1. HPLC Analysis

The composition of each TA sample was determined by reversed phase HPLC. A Hewlett-Packard 1100 gradient HPLC system with an autosampler and a diode array detector was equipped with an Agilent Zorbax C-8 column, 4.6 mm × 150 mm with 5-micron packing (Agilent, Santa Clara, CA, USA). The gradient program employed 0.13% (*v*/*v*) trifluoroacetic acid (TFA) in nanopure water (A) and 0.10% (*v*/*v*) TFA in HPLC-grade acetonitrile (B) at a flow rate of 0.5 mL/min. The 60 min runs were programed as follows: 0–3 min, isocratic at 10% B; 3–40 min, increase to 30% B; 40–50 min, increase to 80% B; 50–55 min, decrease to 10% B, and re-equilibrate. The detector was set at 220 nm and data were collected and processed using ChemStation Rev. A.09.03 software (Agilent, Santa Clara, CA, USA).

2.2.2. Polyphenol Precipitability by Protein

The protein precipitability of the polyphenols in each TA sample was determined using BSA as a model protein [26]. Various amounts of TA ranging from 0 to 100 μg were added to 400 μL of pH 5.9 acetate buffer containing 25 μg of BSA. The solutions were mixed, incubated at room temperature for 30 min, and centrifuged for 5 min at 12,000× *g*. The supernatants were removed by aspiration and the pellets were redissolved in 800 μL of 1% (*m*/*v*) sodium dodecyl sulfate (SDS)/5% (*v*/*v*) triethanolamine solution before adding 200 μL of 0.01 M ferric ammonium sulfate in 0.01 M HCl. The absorbance of each sample at 510 nm was determined and converted to mass of TA precipitated using a calibration plot prepared for each TA (Supplementary Figure S1).

2.2.3. Nanoparticle Synthesis

Slightly different procedures were used to produce uncoated hollow ZNP or hollow ZNP coated with each of the TA preparations [7]. In order to synthesize 2.0 mL of ZNP, 50 μL of either 70% ethanol (uncoated nanoparticles) or 25 mg/mL TA in 70% ethanol (coated nanoparticles) was added to a 500 μL of 70% ethanol containing 30 mg/mL zein. After rotating at room temperature for 30 min, 450 μL of Na_2CO_3 suspended in 70% ethanol (13 mg/mL) was added to the reaction mixture and rotated for 15 min. Finally, an equal volume of nanopure water (1.0 mL) was added and the samples were rotated for another 30 min before centrifuging for 15 min at 5000× *g*. We noted that there was more sediment in the samples of coated ZNP, consistent with the susceptibility of zein to precipitation by tannin [27]. We estimated that 33% more protein was incorporated into uncoated ZNP than into the coated ZNP. The supernatant contained the ZNP suspended in a solution of 2.9 mg/mL Na_2CO_3 in 35% ethanol. The particles were analyzed within 24 h of preparation. The ZNP medium that was used to dilute samples for various analyses was made up of 2.9 mg/mL Na_2CO_3 dissolved in 35% ethanol.

2.2.4. Dynamic Light Scattering

Dynamic light scattering (DLS) measurements were used to determine the hydrodynamic diameter and the polydispersity index (PDI) of the uncoated and coated ZNP. The analyses were performed on a Zetasizer Nano Series (Malvern Panalytical Ltd., Malvern, UK) at 25 °C in disposable 40 μL cuvettes with three averaged instrument runs per sample. Zeta potential was measured using a Zeta Analyzer (Brookhaven Instrument Corp., Holtsville, NY, USA) with six averaged instrument runs per sample. To minimize multiple scattering, samples were diluted with ZNP medium, using a 10-fold dilution for DLS measurements and a 32-fold dilution for zeta potential measurements. The Zetasizer Nano Series instrument collects data at 90°. Instrument parameters such as viscosity and refractive index appropriate for the ZNP medium were used [28,29]. For each measurement three independent samples were analyzed. Data were analyzed with Zetaziser Nano software v 3.30 supplied by Malvern Panalytical Ltd.

2.2.5. Infrared Spectrometry

Coated and uncoated ZNP samples were dried in a speed vacuum concentrator. The dried sample was washed with 35% ethanol and re-dried. The dry, powdered sample was placed on the surface of the crystal in the Perkin Elmer Spectrum One Fourier transform infrared (FT-IR) spectrometer (Shelton, CT, USA) in order to obtain spectra over the wavelength range from 400 cm^{-1} to 4000 cm^{-1}. Spectra of pure zein, pure TA, uncoated ZNP, and coated ZNP were obtained.

2.2.6. Scanning Electron Microscopy

Samples were prepared for scanning electron microscopy (SEM) by depositing a drop of the coated or uncoated ZNP suspension on a clean cover slip mounted on an aluminum stub with adhesive tabs and air drying the sample for 30 min. The stub was then silver painted, and sputter coated with approximately 20 nm of gold. Secondary

electron imaging of each sample was conducted on a Zeiss Supra 35 VP FEG (Baden-Wurttemberg, Germany). All images were taken at 5 KV with an 11.0 mm working distance and magnification varied from 5K times to 95K times for each micrograph. In order to calculate the average particle diameter for each image, the diameter of every particle within the same area was determined and averaged (Supplementary Figure S2).

2.2.7. Circular Dichromsim Spectrometry

Circular dichroism spectra were obtained with an Aviv CD Spectrometer model 435 (Lakewood, NJ, USA). Coated and uncoated ZNP suspensions were diluted 10 times using ZNP medium and transferred to the cuvette (1 mm pathlength) for analysis at 25 °C. Three scans were collected for each sample, and the signal was averaged from 195 nm to 260 nm with an averaging time of 3.0 s, and a settling time of 0.333 s. The ellipticity in millidegrees (mdeg) from three independent determinations was averaged, the background (buffer containing the appropriate TA) was subtracted, and the data were scaled to the uncoated ZNP value 222 nm [30]. The spectra were quantitatively analyzed using the Bestsel algorithm (https://bestsel.elte.hu/index.php (accessed on 10 March 2024)).

2.2.8. Nanoparticle Digestibility

Digestibility was assessed in an in vitro system. The alkaline pH of the ZNP medium was unfavorable for pepsin digestion. The limited trypsin digestibility of zein (5 cleavage sites) led us to focus on chymotrypsin (67 cleavage sites) for our digestion system (cleavage sites predicted for Q00919_MAIZE using PeptideCutter from Expasy https://web.expasy.org/peptide_cutter/ (accessed on 10 March 2024)). The suspension of coated or uncoated ZNPs was diluted with ZNP medium and placed under a stream of nitrogen to remove ethanol from the sample because ethanol inhibits chymotrypsin [31]. To accommodate the lower protein incorporation in coated ZNP, we used 300 µL of coated ZNP diluted with 100 µL of medium, or 200 µL of uncoated ZNP diluted with 200 µL of medium. After removing the ethanol, 120 µL of water and 20 µL of 3M Tris HCl (pH 8) was added to each sample. Chymotrypsin (1.25 mg/mL dissolved in 1 mM HCl containing 2 mM $CaCl_2$) was added to each sample (10 µL) and the samples were incubated at room temperature for 1 h. Digestion was stopped by adding 10 µL of the inhibitor AEBSF (9.6 mg/mL in water). Undigested controls were prepared by adding 10 µL of AEBSF before adding chymotrypsin. After the digestion step, 160 µL of denaturation solution (SDS, β-mercaptoethanol, glycerol and Coomassie blue G-250 as a tracking dye) was added to each sample, and the samples were heated at 100 °C for 10 min. The samples (10 µL) were run on 14% Tris/Tricine SDS-PAGE gel (37.5:1 acrylamide to bis) [32]. Gels were fixed by soaking for 15 min in 12.5% trichloroacetic acid (TCA) in water, then stained with Coomassie stain overnight followed by destaining in 12.5% TCA solution. Zein was the dominant band at about 20kD in digested and undigested samples, with no interference from chymotrypsin which was below the limit of detection. Images were obtained using the ChemiDoc Imaging system (Bio-Rad 3.0.1.14) and were analyzed with ImageJ software (ImageJ.org, National Institute of Health). Five independent preparations of ZNP were digested to obtain average digestibility for each treatment.

2.2.9. Statistical Analysis

Particle size, polydispersity, zeta potential and digestibility data were analyzed with the one-tailed Mann–Whitney test for significance using GraphPad Prism 5. The data were presented as mean and standard error of mean.

3. Results and Discussion

3.1. Characterization of Tannic Acids

Commercially available TA is a mixture of related compounds that have various degrees of galloylation and patterns of substitution (Figure 1) [21,22]. A well-characterized sample of TA was used to correlate HPLC elution time with degree of esterification [22]

(Supplementary Figure S3). We categorized four commercial preparations of TA as short chain length, mixed chain length, or long chain length TA (Figure 2, Table 1). The mixture of isomers in MAL is predominantly mono- to tetra galloyl glucose (1–4 GG), so it is defined as a short chain length TA. ACR and GFS are both dominated by isomers with chain lengths ranging from 5 to 8 galloyl glucose (5–8 GG) and are assigned as long chain length TA. FIS has an equal distribution of shorter and longer chain isomers and is designated as a mixed chain length TA. Pentagalloyl glucose is a purified, defined TA with a fully esterified core sugar.

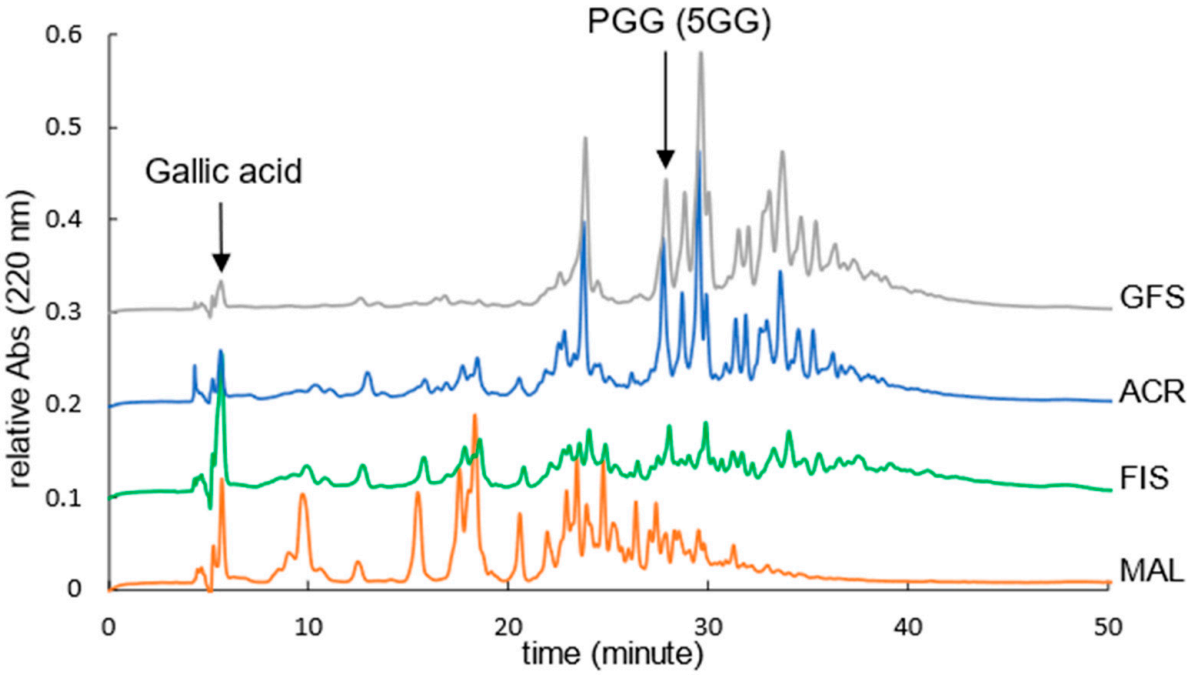

Figure 2. Reversed phase HPLC chromatograms for MAL, FIS, ACR, and GFS tannic acids. Hydrolyzable tannins from different suppliers were run on a C-8 column with a trifluoroacetic acid-modified water/acetonitrile gradient. Arrows indicate the elution times of pure gallic acid and PGG. Tannic acids were obtained from several suppliers: ACR was from Acros Organics (Geel, Belgium), MAL was from Mallinckrodt Chemicals (Paris, KY, USA), GFS was from GFS Chemicals (Powell, OH, USA), and FIS was from Fisher Scientific (Fairlawn, NJ, USA). Pentagalloyl glucose (PGG) was prepared in-house.

Table 1. Percentage of each size class of galloyl esters in the tannic acid preparations.

	Tannic Acid Preparation			
	MAL	**FIS**	**ACR**	**GFS**
% of 1–4 GG [1]	83	51	35	23
% of 5–8 GG [1]	17	49	65	77
Chain length [2]	Short	Mixed	Long	Long

[1] Percent galloyl glucose (GG) was calculated based on peak areas after assigning the peak families using the calibration plot (Supplementary Figure S3). [2] Chain length categories are based on the distribution of material between <5GG and >5GG for each type of TA.

The different preparations of TA had different abilities to precipitate with protein. Tannins bind protein by a combination of hydrogen bonding, hydrophobic and sometimes covalent interactions [12,13]. The tannin–protein complexes precipitate under favorable conditions of tannin-to-protein ratio, pH, solvent composition, and temperature [33]. The tendency to precipitate can easily be measured using a standard protein to determine the percent of added polyphenol that can be precipitated (protein precipitability) [26,33].

A limitation of the method is its dependence on the highly water-soluble model protein BSA, which may not be directly relevant to interactions with protein such as the very hydrophobic zein.

The two long chain TA preparations and PGG were highly precipitable, with about 70% of the added TA co-precipitating with protein (Supplementary Figure S1). The mixed chain length TA (FIS) was also highly precipitable (60%) but only after a threshold level of TA was added to the protein sample (Supplementary Figure S1). The short chain length sample (MAL) was less precipitable (48%) and required a high threshold level of TA to initiate precipitation (Supplementary Figure S1). Our data are very similar to an earlier systematic study of protein precipitability of purified hydrolzyable tannins, in which 80–100% of the octagalloyl glucose (long chain) was precipitated at all tannin-to-protein ratios, but less than 40% of the trigalloyl glucose (short chain) was precipitated at the best ratio [23]. Long-chain TA preparations appear to efficiently form multivalent crosslinks between BSA molecules and co-precipitate with the protein [23]. Short chain TA may bind to the protein but do not form crosslinks, limiting precipitation [33]. The precipitability data and the chain length assignments highlight the unique characteristics of different preparations of TA that we used to coat ZNP.

3.2. Size, PDI and Zeta Potential of Zein Nanoparticles

The diameters of the uncoated ZNP (Table 2) were as much as three times larger than the diameters previously reported for solid ZNP [34] or hollow ZNP [6,35]. The high concentration of Na_2CO_3 (2–9%) used to form the template in earlier studies of hollow ZNP probably promoted rapid precipitation of the carbonate and thus small template particles and small ZNP. We used a lower concentration of Na_2CO_3 (1.3%) that may have precipitated more slowly to form larger templates and thus larger ZNP. A study of how carbonate concentration affects particle size would be useful for future applications of the anti-solvent process.

Table 2. Diameter, PDI and zeta potential of coated or uncoated zein nanoparticles determined by DLS.

Coating	Diameter [1] (nm)	PDI [1]	Zeta Potential [1] (mV)
Uncoated	200 ± 4	0.082 ± 0.012	−26.7 ± 0.3
MAL (short)	189 ± 3	0.044 ± 0.011 *	−33.7 ± 0.3 **
FIS (mixed)	186 ± 1 **	0.048 ± 0.010	−36.0 ± 0.6 **
PGG (pure)	185 ± 1 **	0.046 ± 0.019	−36.7 ± 0.3 **
ACR (long)	179 ± 0 **	0.047 ± 0.017	−35.3 ± 0.7 **
GFS (long)	183 ± 1 **	0.062 ± 0.023	−35.0 ± 1.5 **

[1] The means and standard errors of mean are shown (n = 3). Statistical comparisons to the mean are indicated by * $p < 0.1$, ** $p < 0.05$.

Our TA-coated ZNP are more compact than uncoated ZNP (Table 2). In comparison to some earlier studies in which the TA coating minimally reduced the size of the particles (92 nm vs. 88 nm diameter) [7], our TA coatings reduced particle diameter by around 8% compared to uncoated particles (Table 2). Coating with a short chain length TA tended to reduce the particle size ($p = 0.100$) but the effect was greater and reached significance ($p < 0.05$) for the mixed chain length TA, long chain length TA, or pure PGG. The reduced particle size is consistent with the multivalent nature of long chain TA, allowing it to bind zein at several sites resulting in crosslinks that pull proteins close together and shrink the ZNP.

Uncoated hollow ZNP have a homogeneous size distribution with acceptable PDI values (Table 2). Although some authors report that coating hollow ZNP with TA slightly increases the PDI [7], we found that coating the particles with TA tended to decrease polydispersity (Table 2). Particles coated with long or mixed chain length TA or with PGG are slightly less polydisperse than uncoated particles, but particles coated with short chain

length TA were significantly less polydisperse ($p < 0.1$, Table 2). This effect of MAL is consistent with the limited precipitation ability of this TA. Short-chain TA may add a polar coat to the ZNP but do not bind at multiple sites and are unable to crosslink the protein, thus preventing aggregation and yielding a more homogeneous population of particles.

The zeta potentials of the coated ZNP were significantly more negative than those of the uncoated ZNP (Table 2), similar to earlier reports [7]. The zeta potential is dictated by the pH of the solution and the pKa values for functional groups on the surface of the particle. The ZNP medium has a pH of about 10, well above the pI of zein (pI~6), so ZNP typically have a negative surface charge [35] similar to our uncoated ZNP (Table 2). The pH of the ZNP medium for coated nanoparticles is about 8, because during particle synthesis the weakly acidic TA neutralizes some of the carbonate in the solution. The many phenolic functional groups of TA are about half protonated at pH 8 (pKa~7.8) [36], so the TA coat contributes additional negative charge beyond that of the zein, resulting in a more negative zeta potential for all of the coated ZNP (Table 2). In principle, a more negative zeta potential is associated with less aggregation and increased stability of particle suspensions, leading us to believe that TA may stabilize ZNP.

3.3. Intermolecular Interactions between Zein and TA in Zein Nanoparticles

The FT-IR spectra of zein and of TA were similar to published spectra [37–39]. The spectrum of uncoated ZNP was almost indistinguishable from that of pure zein (Figure 3). The spectra of ZNP coated with any type of TA had features of both zein and TA, confirming incorporation of TA into the particles [7]. For example, the 1203 cm^{-1} band due to aromatic esters is clearly visible in the spectra of TA or coated ZNP, but not in pure zein or uncoated ZNP (Figure 3). The aryl C-H bending band at 750 cm^{-1} is present in spectrum of TA and the spectra of TA-coated ZNP (Figure 3).

There were no clear differences between the spectra from ZNP made with the different preparations of TA, consistent with the structural variation in number but not types of functional groups in the different types of TA. In some regions, the protein signals overwhelmed the TA signals suggesting close interactions between the TA and protein [40]. For example, the TA aromatic C-O stretch (1609 cm^{-1}) and the TA phenolic ester stretch (1698 cm^{-1}) are both obscured by the strong amide carbonyl band at 1645 cm^{-1} contributed by the protein (Figure 3). The >3000 cm^{-1} region of the zein spectrum has a distinct band centered at 3291 cm^{-1} but the TA control has a broad band in the same region (Figure 3). These bands are attributed to the amide nitrogen stretch and inter- and intra-molecular hydrogen bonding of phenolic OH groups, respectively. Loss of the signal typical of phenolic hydrogen bonds in the TA-coated ZNP may be indicative of TA-amide hydrogen bonding in the ZNP. The strong spectral band attributed to aromatic C-O bending (1310 cm^{-1}) is distinct in the TA control but is barely visible in the coated ZNP spectra (Figure 3), providing additional support for the idea that the phenolic OH groups are involved in the TA–zein interaction that forms the ZNP coat. The strong TA signals at 1195 cm^{-1}, 1080 cm^{-1} and 1019 cm^{-1} are attributed to C-O stretching (Figure 3). Each of these bands appears to have shifted slightly to 1203 cm^{-1}, 1120 cm^{-1} and 1046 cm^{-1} in the coated particles, again pointing to changes in the TA when it coats the ZNP.

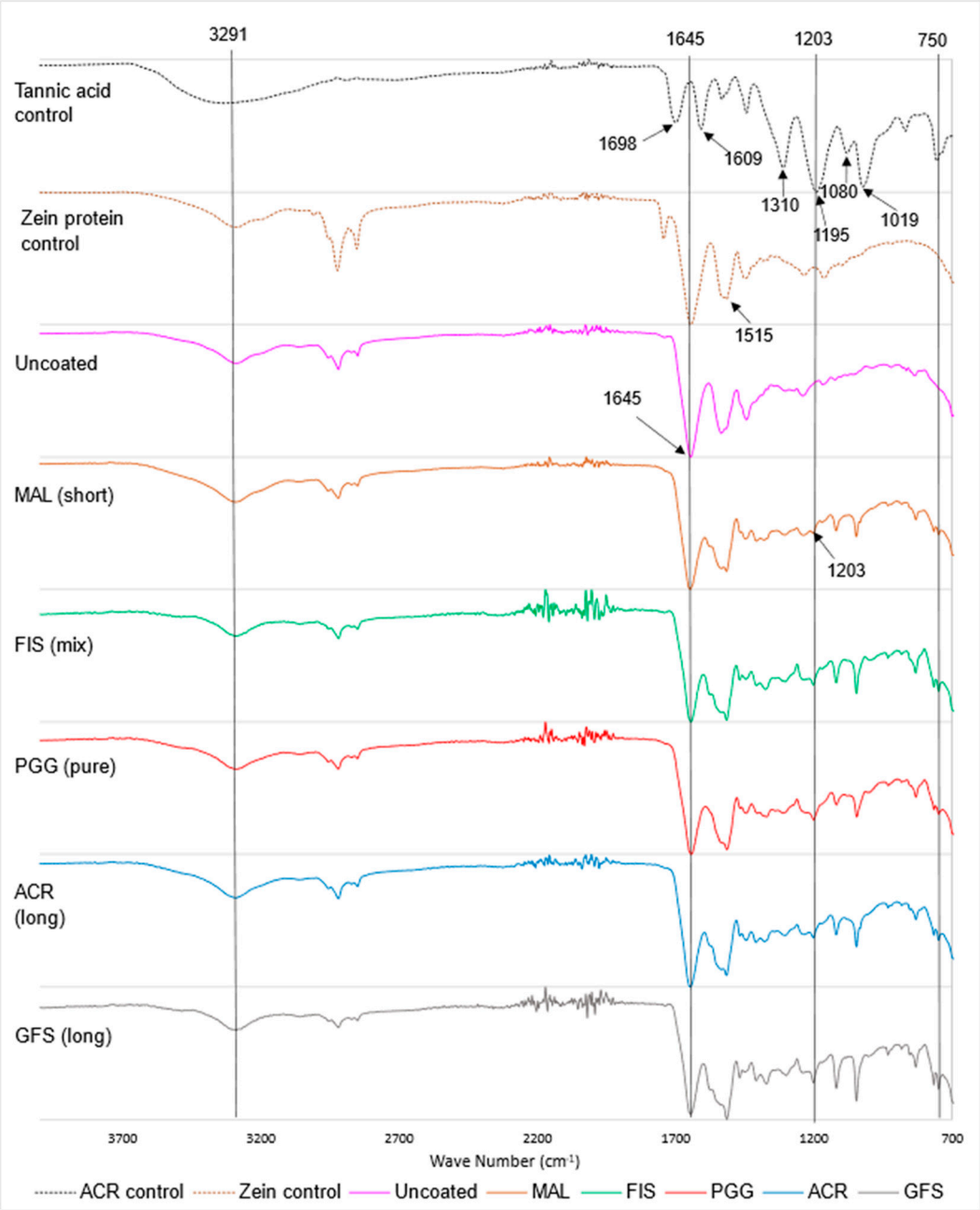

Figure 3. FT-IR spectra of tannic acid control, zein control, and coated or uncoated zein nanoparticles. The wavenumbers corresponding to important functional groups are labeled.

3.4. Morphology of Zein Nanoparticles

During the process of drying the samples for SEM, the uncoated ZNP form irregular aggregates of highly textured particles (Figure 4a). The TA-coated ZNPs have smooth surfaces and are arranged like beads on a string (Figure 4b–f). For MAL and FIS, the images reveal small groups and chains of particles that are only two to three particles wide (Figure 4b,c). Zein nanoparticles coated with PGG, ACR or GFS form longer chains that may be four to five particles wide (Figure 4d–f). For each type of ZNP, the size of the individual particles determined by SEM (Table 3) is about 25% smaller than the size determined by DLS (Table 2), because SEM reveals the size of the dry particle while DLS provides the hydrodynamic size of the fully hydrated ZNP. For the SEM measurements, the uncoated particles are larger than the coated particles (Table 3), with the difference reaching significance for the ZNP coated with pure PGG or long chain TA (Table 3). The

tendency of long galloyl chain TA to decrease the size of the ZNP is consistent for the DLS and the SEM determinations.

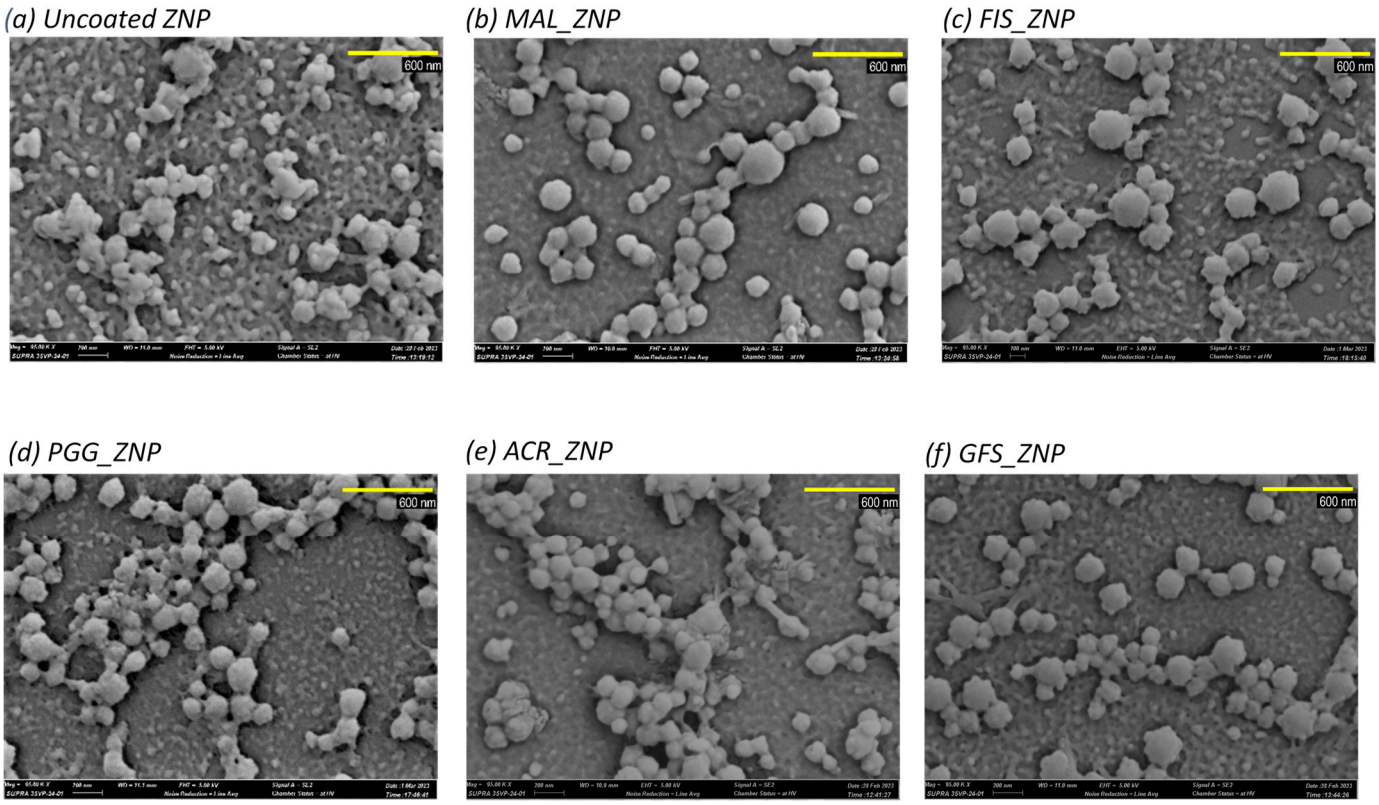

Figure 4. Scanning electron microscopy images of (**a**) uncoated ZNP, (**b**) ZNP coated with MAL (short), (**c**) ZNP coated with FIS (mixed), (**d**) ZNP coated with PGG (pure), (**e**) ZNP coated with ACR (long), (**f**) ZNP coated with GFS (long). The yellow bars in each panel represents 600 nm.

Table 3. Average zein nanoparticle size determined from the scanning electron microscopy images.

Coating	Diameter (nm) [1]
Uncoated	156 ± 7
MAL (short)	145 ± 4
FIS (mixed)	151 ± 5
PGG (pure)	136 ± 4 ***
ACR (long)	134 ± 4 ***
GFS (long)	140 ± 5 ***

[1] The values are the average +/− standard error of mean for n = 48–96 particles found in a grid of 5.92 mm^2 (Supplementary Figure S2). Statistical comparisons to the mean are indicated by *** $p < 0.001$.

3.5. Protein Secondary Structure in Zein Nanoparticles

The secondary structure of the protein in ZNP was not changed by coating the particles with TA (Figure 5). The CD spectra of either uncoated or coated ZNP had negative peaks at 208 and 222 nm, indicating some α-helical elements in the protein. The literature suggested that forming the nanoparticles would increase β-sheet and random coil elements compared to the 50–60% α-helix typical of native zein under favorable dissolution conditions of 70% ethanol [41–43]. We analyzed our spectra with the Bestsel web-based algorithm (https://bestsel.elte.hu/index.php (accessed on 10 March 2024)), which is used to optimize detection of β-structures [30] (Supplementary Table S1). The quantitative analysis indicated that less than 10% of the secondary structure of zein in ZNP comprised α-helices. Beta structures (25%), turns (15%) and unordered regions (50%) dominated the protein structure in the ZNP with no effect of coating the particles with TA of any chain length (Supplementary

Table S1). Data from other authors for ZNP were similar to our data, with loss of helical structure relative to the native protein [43]. Although increasing solvent polarity decreases helical structure in zein [41], the dominant effect on structure for ZNP appears to be protein aggregation and packing. The effect of solvent on the structure was relatively limited, with about 40% helical structure for zein in 45% ethanol compared to 10% for ZNP in 35% ethanol (Supplementary Table S1).

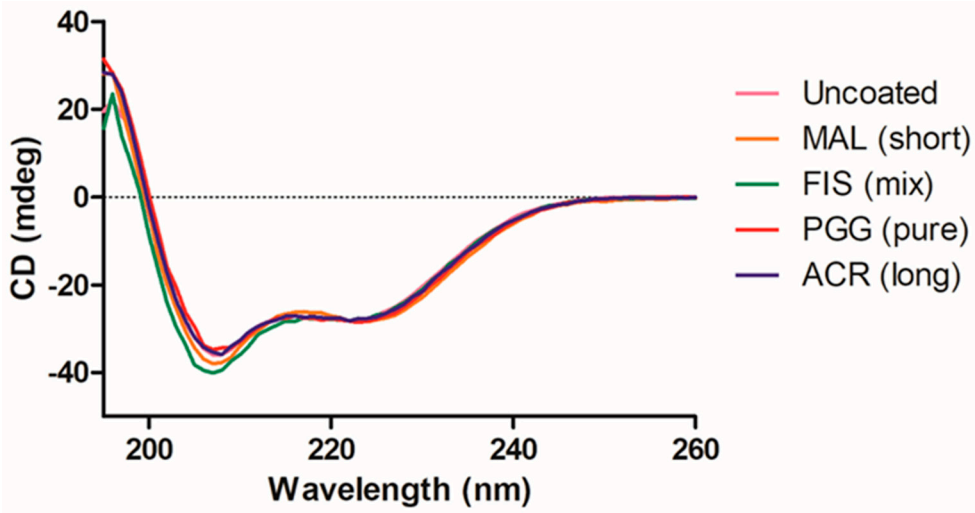

Figure 5. Circular dichroism spectra of coated or uncoated zein nanoparticles. Each line represents the average spectrum based on three independent samples. The background with the appropriate TA was subtracted and the data were scaled to the signal at 222 nm for the uncoated ZNP.

3.6. Digestibility of Zein Nanoparticles

Zein is a protein with low digestibility due to its high disulfide content and preponderance of hydrophobic residues [9]. We optimized a simple in vitro system that used SDS-PAGE to monitor loss of the 20 kD zein band after chymotrypsin digestion. Replication of the integrated peak areas was poor with errors as large as 30% of the mean (Table 4), but differences between the TA treatments could be discerned. Under the optimized conditions, about 40% of the uncoated ZNP sample was digested (Table 4). Digestibility of ZNP was not affected when the particles were coated with long chain length tannic acids (Table 4). Pure PGG-coated ZNP tended to be less digestible than the uncoated ZNP, but the change did not reach significance (Table 4). In contrast, coating the ZNP with short chain length TA significantly increased digestibility of the particles, and mixed chain length TA similarly tended to increase digestibility (Table 4).

Table 4. Average % digestion of coated or uncoated zein nanoparticles by chymotrypsin.

Coating	Average Digestion (%) [1]
Uncoated	42.8 ± 6.5
MAL (short)	62.4 ± 5.5 **
FIS (mixed)	54.9 ± 13.8
PGG (pure)	29.7 ± 7.5
ACR (long)	40.4 ± 4.4
GFS (long)	40.7 ± 12.6

[1] Average +/− standard error of mean (n = 5). Statistical comparisons to the mean are indicated by ** $p < 0.05$.

The digestibility results were surprising in light of the well-established dogma that tannin is a universal enzyme inhibitor [44]. However, there is little opportunity for the nanoparticle-bound TA to interact with the soluble enzyme, so it is likely that the TA does not directly inhibit the enzyme in this system. The long chain TA that were the most efficient protein precipitating agents tended to decrease (PGG) or not change (ACR, GFS)

ZNP digestibility, suggesting that the enzyme was able to access the TA-substrate complex, with regions of the zein that were not directly bound to the TA being susceptible to cleavage. Based on the increased digestibility of ZNP coated with short or mixed chain length TA, we suggest that a redox chemistry mechanism has the most important impact on digestibility of TA-coated ZNP. We propose that TA acts on zein as a reducing agent, converting disulfide bonds to thiols and increasing zein digestibility [45,46]. The oxidative activity of short chain TA is higher than that of long chain TA [47], making MAL and FIS better candidates to reduce disulfides and increase digestibility, consistent with our data. We suggest that TA with specific protein binding and redox properties could be used to "tune" the digestibility of ZNP or other thiol-rich proteins for specific applications.

4. Conclusions

We conclude that variability of galloyl ester chain length for different preparations of TA can influence the structural and functional features of zein protein nanoparticles coated with TA. This effect was reflected in our data relevant to size, polydispersity index, zeta potential, morphology, and digestibility. Coating the ZNP with any TA increased the surface charge (zeta potential) and increased surface uniformity of the nanoparticles regardless of the TA chain length. However, the chain length of the galloyl esters influenced size of the ZNP and the digestibility of the protein nanoparticles. Thus, TA could be used to optimize the properties of ZNP for different applications. For example, it may be favorable to use particles with increased digestibility (short chain TA coating) for some cargos. For other applications, it may be desirable to create particles with minimal size (long chain TA coat). Future work includes extending this work to coating the particles with condensed tannins as well as loading particles with drugs to more fully explore how polyphenol coatings can be used to obtain protein nanoparticles with the best combination of properties for any application.

Supplementary Materials: The following supporting information can be downloaded at: https://www.mdpi.com/article/10.3390/compounds4020024/s1, Figure S1: Protein precipitability of the TA preparations; Figure S2: Example of diameter determination from SEM images; Figure S3. HPLC calibration plot developed with a well-characterized sample of TA and purified standard galloyl esters; Table S1. Quantitative analysis of native zein and ZNP secondary structures.

Author Contributions: Conceptualization, A.E.H.; methodology, S.Y.M.; formal analysis, A.E.H. and S.Y.M.; investigation, S.Y.M., N.C.R. and E.G.; resources, A.E.H.; data curation, A.E.H.; writing—original draft preparation, S.Y.M.; writing—review and editing, A.E.H.; visualization, S.Y.M.; supervision, A.E.H.; project administration, A.E.H.; funding acquisition, A.E.H. All authors have read and agreed to the published version of the manuscript.

Funding: This work was funded by National Science Foundation, subcontract to AEH from Grant Number 1750189 to Kelly C. Wrighton, Colorado State University.

Data Availability Statement: The raw data supporting the conclusions of this article will be made available by the authors on request.

Conflicts of Interest: The authors declare no conflicts of interest.

References

1. Lai, L.F.; Guo, H.X. Preparation of new 5-fluorouracil-loaded zein nanoparticles for liver targeting. *Int. J. Pharm.* **2011**, *404*, 317–323. [CrossRef]
2. Jahanshahi, M.; Babaei, Z. Protein nanoparticle: A unique system as drug delivery vehicles. *Afr. J. Biotech.* **2008**, *7*, 4926–4934.
3. Redhead, H.M.; Davis, S.S.; Illum, L. Drug delivery in poly(lactide-co-glycolide) nanoparticles surface modified with poloxamer 407 and poloxamine 908: In vitro characterisation and in vivo evaluation. *J. Control. Release* **2001**, *70*, 353–363. [CrossRef]
4. Esfanjani, A.F.; Jafari, S.M. Biopolymer nano-particles and natural nano-carriers for nano-encapsulation of phenolic compounds. *Colloid Surf. B-Biointerfaces* **2016**, *146*, 532–543. [CrossRef]
5. Jia, C.S.; Cao, D.D.; Ji, S.P.; Zhang, X.M.; Muhoza, B. Tannic acid-assisted cross-linked nanoparticles as a delivery system of eugenol: The characterization, thermal degradation and antioxidant properties. *Food Hydrocoll.* **2020**, *104*, 105717. [CrossRef]

6. Xu, H.L.; Jiang, Q.R.; Reddy, N.; Yang, Y.Q. Hollow nanoparticles from zein for potential medical applications. *J. Mater. Chem.* **2011**, *21*, 18227–18235. [CrossRef]
7. Hu, S.Q.; Wang, T.R.; Fernandez, M.L.; Luo, Y.C. Development of tannic acid cross-linked hollow zein nanoparticles as potential oral delivery vehicles for curcumin. *Food Hydrocoll.* **2016**, *61*, 821–831. [CrossRef]
8. Wang, Y.; Padua, G.W. Nanoscale characterization of zein self-assembly. *Langmuir* **2012**, *28*, 2429–2435. [CrossRef]
9. Lee, S.H.; Hamaker, B.R. Cys155 of 27 kda maize gamma-zein is a key amino acid to improve its in vitro digestibility. *FEBS Lett.* **2006**, *580*, 5803–5806. [CrossRef]
10. Luo, Y.C.; Teng, Z.; Wang, Q. Development of zein nanoparticles coated with carboxymethyl chitosn for encapsulation and controlled release of vitamin d3. *J. Agric. Food Chem.* **2012**, *60*, 836–843. [CrossRef]
11. Luo, Y.C.; Zhang, B.C.; Whent, M.; Yu, L.L.; Wang, Q. Preparation and characterization of zein/chitosan complex for encapsulation of alpha-tocopherol, and its in vitro controlled release study. *Colloid Surf. B-Biointerfaces* **2011**, *85*, 145–152. [CrossRef]
12. Hagerman, A.E. Fifty years of polyphenol-protein complexes. *Rec. Adv. Polyphen. Res.* **2012**, *3*, 71–97.
13. Pizzi, A. Covalent and ionic bonding between tannin and collagen in leather-making and shrinking: A MALDI-Tof study. *J. Renew. Mat.* **2021**, *9*, 1345–1364. [CrossRef]
14. Aron, P.M.; Shellhammer, T.H. A discussion of polyphenols in beer physical and flavour stability. *J. Inst. Brew.* **2010**, *116*, 369–380. [CrossRef]
15. Baldwin, A.; Booth, B.W. Biomedical applications of tannic acid. *J. Biomater. Appl.* **2022**, *36*, 1503–1523. [CrossRef]
16. Al-Hijazeen, M.; Lee, E.J.; Mendonca, A.; Ahn, D.U. Effects of tannic acid on lipid and protein oxidation, color, and volatiles of raw and cooked chicken breast meat during storage. *Antioxidants* **2016**, *5*, 19. [CrossRef]
17. Chen, Y.-N.; Jiao, C.; Zhao, Y.; Zhang, J.; Wang, H. Self-assembled polyvinyl alcohol–tannic acid hydrogels with diverse microstructures and good mechanical properties. *ACS Omega* **2018**, *3*, 11788–11795. [CrossRef]
18. Zhou, L.; Chen, M.; Tian, L.; Guan, Y.; Zhang, Y. Release of polyphenolic drugs from dynamically bonded layer-by-layer films. *ACS Appl. Mater. Interfaces* **2013**, *5*, 3541–3548. [CrossRef]
19. Gulcin, I.; Huyut, Z.; Elmastas, M.; Aboul-Enein, H.Y. Radical scavenging and antioxidant activity of tannic acid. *Arab. J. Chem.* **2010**, *3*, 43–53. [CrossRef]
20. Daglia, M. Polyphenols as antimicrobial agents. *Curr. Opin. Biotechnol.* **2012**, *23*, 174–181. [CrossRef]
21. Pizzi, A.; Pasch, H.; Giovando, S. Polymer structure of commercial hydrolyzable tannins by matrix-assisted laser desorption/ionization-time-of flight mass spectrometry. *J. Appl. Polym. Sci.* **2009**, *113*, 3847–3859. [CrossRef]
22. Kinraide, T.; Hagerman, A.E. Interactive intoxicating and ameliorating effects of tannic acid, aluminum (Al^{3+}), copper (Cu^{2+}) and selenate (SeO_4^{2-}) in wheat roots. A descriptive and mathematical assessment. *Physiol. Plant.* **2010**, *139*, 68–79. [CrossRef]
23. Engstrom, M.T.; Virtanen, V.; Salminen, J.-P. Influence of the hydrolyzable tannin structure on the characteristics of insoluble hydrolyzable tannin-protein complexes. *J. Agric. Food Chem.* **2022**, *70*, 13036–13048. [CrossRef]
24. Gross, G.G. From lignins to tannins: Forty years of enzyme studies on the biosynthesis of phenolic compounds. *Phytochemistry* **2008**, *69*, 3018–3031. [CrossRef]
25. Chen, Y.; Hagerman, A.E. Characterization of soluble non-covalent complexes between bovine serum albumin and beta-1,2,3,4,6-penta-O-galloyl-d-glucopyranose by MALDI-TOF MS. *J. Agric. Food Chem.* **2004**, *52*, 4008–4011. [CrossRef]
26. Hagerman, A.E.; Butler, L.G. Protein precipitation method for the quantitative determination of tannins. *J. Agric. Food Chem.* **1978**, *26*, 809–812. [CrossRef]
27. Simonato, B.; Mainente, F.; Selvatico, E.; Violoni, M.; Pasini, G. Assessment of the fining efficiency of zeins extracted from commercial corn gluten and sensory analysis of the treated wine. *LWT-Food Sci. Technol.* **2013**, *54*, 549–556. [CrossRef]
28. Scott, T.A. Refractive index of ethanol-water mixtures and density and refractive index of ethanol-water-ethyl ether mixtures. *J. Phys. Chem.* **1946**, *50*, 406–412. [CrossRef]
29. Anonymous Viscosity of Two Component Mixtures. Available online: https://www.rheosense.com/applications/viscosity/two-component-mixtures (accessed on 22 November 2023).
30. Miles, A.J.; Janes, R.W.; Wallace, B.A. Tools and methods for circular dichroism spectroscopy of proteins: A tutorial review. *Chem. Soc. Rev.* **2021**, *50*, 8400–8413. [CrossRef]
31. Sato, M.; Sasaki, T.; Kobayashi, M.; Kise, H. Time-dependent structure and activity changes of alpha-chymotrypsin in water/alcohol mixed solvents. *Biosci. Biotechnol. Biochem.* **2000**, *64*, 2552–2558. [CrossRef]
32. Schagger, H. Electrophoretic isolation of membrane-proteins from acrylamide gels. *Appl. Biochem. Biotechnol.* **1994**, *48*, 185–203. [CrossRef]
33. Hagerman, A.E.; Rice, M.E.; Ritchard, N.T. Mechanisms of protein precipitation for two tannins, pentagalloyl glucose and epicatechin$_{16}$ (4 → 8) catechin (procyanidin). *J. Agric. Food Chem.* **1998**, *46*, 2590–2595. [CrossRef]
34. Liu, Q.G.; Jing, Y.Q.; Han, C.P.; Zhang, H.; Tian, Y.M. Encapsulation of curcumin in zein/caseinate/sodium alginate nanoparticles with improved physicochemical and controlled release properties. *Food Hydrocoll.* **2019**, *93*, 432–442. [CrossRef]
35. Xu, H.L.; Zhang, Y.; Jiang, Q.R.; Reddy, N.; Yang, Y.Q. Biodegradable hollow zein nanoparticles for removal of reactive dyes from wastewater. *J. Environ. Manag.* **2013**, *125*, 33–40. [CrossRef] [PubMed]
36. Ghigo, G.; Berto, S.; Minella, M.; Vione, D.; Alladio, E.; Nurchi, V.M.; Lachowicz, J.; Daniele, P.G. New insights into the protogenic and spectroscopic properties of commercial tannic acid: The role of gallic acid impurities. *New J. Chem.* **2018**, *42*, 7703–7712. [CrossRef]

37. Dai, L.; Sun, C.X.; Wang, D.; Gao, Y.X. The interaction between zein and lecithin in ethanol-water solution and characterization of zein-lecithin composite colloidal nanoparticles. *PLoS ONE* **2016**, *11*, e0167172. [CrossRef] [PubMed]
38. Tangarfa, M.; Semlali Aouragh Hassani, N.; Alaoui, A. Behavior and mechanism of tannic acid adsorption on the calcite surface: Isothermal, kinetic, and thermodynamic studies. *ACS Omega* **2019**, *4*, 19647–19654. [CrossRef] [PubMed]
39. Abd-El Hafeez, S.I.; Eleraky, N.E.; Hafez, E.; Abouelmagd, S.A. Design and optimization of metformin hydrophobic ion pairs for efficient encapsulation in polymeric drug carriers. *Sci. Rep.* **2022**, *12*, 5737. [CrossRef] [PubMed]
40. Zou, Y.; Guo, J.; Yin, S.W.; Wang, J.M.; Yang, X.Q. Pickering emulsion gels prepared by hydrogen-bonded zein/tannic acid complex colloidal particles. *J. Agric. Food Chem.* **2015**, *63*, 7405–7414. [CrossRef]
41. Erickson, D.P.; Ozturk, O.K.; Selling, G.; Chen, F.; Campanella, O.H.; Hamaker, B.R. Corn zein undergoes conformational changes to higher β-sheet content during its self-assembly in an increasingly hydrophilic solvent. *Int. J. Biol. Macromol.* **2020**, *157*, 232–239. [CrossRef]
42. Zhao, S.; Deng, Y.; Yan, T.; Yang, X.; Xu, W.; Liu, D.; Wang, W. Explore the interaction between ellagic acid and zein using multi-spectroscopy analysis and molecular docking. *Foods* **2022**, *11*, 2764. [CrossRef] [PubMed]
43. Wang, X.; Fan, M. Interaction behaviors and structural characteristics of zein/NaTC nanoparticles. *RSC Adv.* **2019**, *9*, 5748–5755. [CrossRef] [PubMed]
44. Samtiya, M.; Aluko, R.E.; Dhewa, T. Plant food anti-nutritional factors and their reduction strategies: An overview. *Food Prod. Process. Nutr.* **2020**, *2*, 6. [CrossRef]
45. Zhang, L.; Cheng, L.B.; Jiang, L.J.; Wang, Y.S.; Yang, G.X.; He, G.Y. Effects of tannic acid on gluten protein structure, dough properties and bread quality of chinese wheat. *J. Sci. Food Agric.* **2010**, *90*, 2462–2468. [CrossRef] [PubMed]
46. Hamaker, B.R.; Kirleis, A.W.; Butler, L.G.; Axtell, J.D.; Mertz, E.T. Improving the in vitro protein digestibility of sorghum with reducing agents. *Proc. Natl. Acad. Sci. USA* **1987**, *84*, 626–628. [CrossRef]
47. Barbehenn, R.V.; Jones, C.P.; Hagerman, A.E.; Karonen, M.; Salminen, J.P. Ellagitannins have greater oxidative activities than condensed tannins and galloyl glucoses at high ph: Potential impact on caterpillars. *J. Chem. Ecol.* **2006**, *32*, 2253–2267. [CrossRef]